REVISTA INTERDISCIPLINAR DE PESQUISA EM ENGENHARIA

CILAMCE 2016

XXXVII IBERIAN LATIN AMERICAN CONGRESS ON COMPUTATIONAL METHODS IN ENGINEERING
BRASÍLIA - DF - BRAZIL

COMPARATIVE STUDY OF THE WEAK-FORM COLLOCATION MESHLESS FORMULATION AND OTHER MESHLESS METHODS

Tiago da Silva Oliveira

Artur Portela

tiago_antuney@hotmail.com

aportela@unb.br

University of Brasília

Department of Civil Engineering, Faculty of Technology, 70910-900, Brasília-DF, Brasil

Abstract. *This paper is concerned with the numerical comparison of the weak-form collocation, a new local meshless method, and other meshless methods, for the solution of two-dimensional problems in linear elasticity. Four methods are compared, namely, the Generalized-Strain Mesh-free (GSMF) formulation, the Rigid-body Displacement Mesh-free (RBDMF) formulation, the Element-free Galerkin (EFG) and the Meshless Local Petrov-Galerkin Finite Volume Method (MLPG FVM). While the RBDMF, EFG and MLPG FVM rely on integration and quadrature process to obtain the stiffness matrix, the GSMF is completely integration free, working as a weighted-residual weak-form collocation. This weak-form collocation readily overcomes the well-known difficulties of the strong-form collocation, such as low accuracy and instability of the solution. A numerical example was analyzed with these methods, in order to assess the accuracy and the computational effort. The results obtained are in agreement with those of the available analytical solution. The numerical results show that the GSMF, when compared to the other methods, is superior not only regarding the computational efficiency, but also regarding the accuracy.*

Keywords: *Local Meshless, Generalized-strain, Weak-form collocation, Local work theorem, Comparative study.*

1 INTRODUCTION

Computer modeling is used to support a broad variety of science and technology areas, simulating the behavior of a real system. Numerical models after successful validation permit advanced design, optimization and control of new components and processes. There are several numerical modeling techniques available nowadays, among which the Finite Element Method (FEM) is the most popular and widely used, mainly for engineers and scientists. Although the method is well established and have a massive influence over the past decades, it still suffers from several downsides. FEM requires the creation of a geometric mesh made of finite elements discretizing the solution domain. It is known that distorted geometry may have a negative impact on the solution accuracy, which means that the mesh becomes a major aspect of FEM. Thus a human-labor intensive process of constructing high quality meshes is required. Other problems of finite element mesh may also appear, for example element locking in modeling slender structures, costly remeshing or element distortion during large deformation analyses.

In order to reduce the labor of creating the finite element mesh and reduce the computational effort, various mesh reduction techniques were researched and developed. Among them, the Meshless methods received the attention of many researchers in a recent past.

Meshfree, or meshless, have some advantages when compared to mesh-based methods. The essential feature of these methods is that they perform the discretization of the problem domain and boundaries with a set of scattered field nodes that do not require any mesh for the approximation of the field variables. In general, their formulation is based in the weighted-residual method, see Finalyson (1972).

Some meshless methods are based on a weighted-residual weak-form formulation. After discretization, the weak form is used to derive a system of algebraic equations through a process of numerical integration using sets of background cells, globally or locally constructed in the domain of the problem. Research on meshfree methods, based on a weighted-residual weak-form formulation, significantly increased after the publication of the Diffuse Element Method (DEM), introduced by Nayroles et al. (1992). The Reproducing Kernel Particle Method (RKPM), presented by Liu et al. (1995), and the Element-free Galerkin (EFG) method, presented by Belytschko et al. (1994), were the first weak-form meshless methods applied in solid mechanics.

All these weak-form meshless methods rely on background cells for the integration of the weighted-residual weak form over the global domain, in the process of the generation of the system of algebraic equations and therefore, they are not truly meshless methods.

In order to overcome the use of a global integration background mesh, a class of meshfree methods based on local weighted-residual weak forms, such as the Meshless Local Petrov–Galerkin (MLPG) method presented by Atluri and Zhu (1998), and also Atluri and Shen (2002), the Meshless Local Boundary Integral Equation (MLBIE) method presented by Zhu et al. (1998), the Local Point Interpolation Method (LPIM) presented by Liu and Gu (2001) and the Local Radial Point Interpolation Method (LRPIM) presented by Liu et al. (2002), have been developed. Among them, the most popular of these methods is the MLPG, based on a moving least-squares (MLS) approximation. The main difference of the MLPG method to other global meshless methods, such as EFG or RKPM, is that local weak forms are used, for integration on overlapping regular-shaped local subdomains, instead of global weak forms and consequently the method does not require the use of a background global mesh, but only a background local

grid which usually has a simple shape.

Atluri et al. (2004) presented an implementation of the meshless Finite Volume Method (FVM), through the MLPG mixed approach, for solving elasto-static problems. In this approach, both the strains and displacements are independently interpolated, at randomly distributed points in the domain, through a local meshless interpolation schemes such as MLS. Then, the nodal values of strains are expressed in terms of the interpolated nodal values of displacements, by simply enforcing the strain-displacement relationships directly by collocation at the nodal points. This formulation eliminates the expensive process of directly differentiating the MLS interpolations for displacements in the entire domain, to compute the strains, leading to a high computational efficiency.

In order to further improve the computational efficiency, two formulations were presented by Oliveira and Portela (2016), the Rigid-body Displacement Mesh-free (RBDMF) formulation and the Generalized-Strain Mesh-free (GSMF) formulation. In the first formulation, the local work theorem leads to a weak form that is a regular local boundary integral equation. In the second formulation, the local work theorem generates a weak form that is completely integration free, working as a weighted-residual weak-form collocation.

This paper is concerned with the numerical comparison of the weak-form collocation and other meshless methods, such as the RBDMF, the EFG and the MLPG FVM, for the solution of two-dimensional problems in linear elasticity. The GSMF performs better than the other meshless methods regarding both computational efficiency and accuracy, as shown in the numerical examples.

2 MLS APPROXIMATION

Let Ω be the domain of a body with boundary Γ and let $N = \{\mathbf{x}_1, \mathbf{x}_2, ..., \mathbf{x}_N\} \in \Omega$ be a set of scattered nodal points that represents a meshless discretization, in which some of them are located on the boundary Γ, as represented in Fig. 1. Circular or rectangular local supports, centered at each nodal point, can be used. In a neighborhood of a sampling point $\mathbf{x}$, the domain of definition of MLS approximation is the subdomain $\Omega_{\mathbf{x}}$, where the approximation is defined.

2.1 Shape Functions

Let $\Omega_{\mathbf{x}}$ be the domain of definition of the MLS approximation, in a neighbourhood of a sampling point $\mathbf{x}$. To approximate the displacement $u(\mathbf{x}) \in \Omega_{\mathbf{x}}$, over a number of scattered nodes $\mathbf{x}_i \in \Omega$, $i = 1, 2, \ldots, n$, where the nodal parameters $\hat{u}_i$ are defined, the MLS approximation is given by

$$u^h(\mathbf{x}) = \mathbf{p}^T(\mathbf{x})\mathbf{a}(\mathbf{x}), \tag{1}$$

for $\mathbf{x} \in \Omega_{\mathbf{x}}$, in which

$$\mathbf{p}^T(\mathbf{x}) = [p_1(\mathbf{x}), p_2(\mathbf{x}), \ldots, p_m(\mathbf{x})], \tag{2}$$

is a vector of the complete monomial basis of order m and $\mathbf{a}(\mathbf{x})$ is the vector of unknown coefficients $a_j(\mathbf{x})$, $j = 1, 2, \ldots, m$ that are functions of the space coordinates $\mathbf{x} = [x_1, x_2]^T$, for 2-D problems.

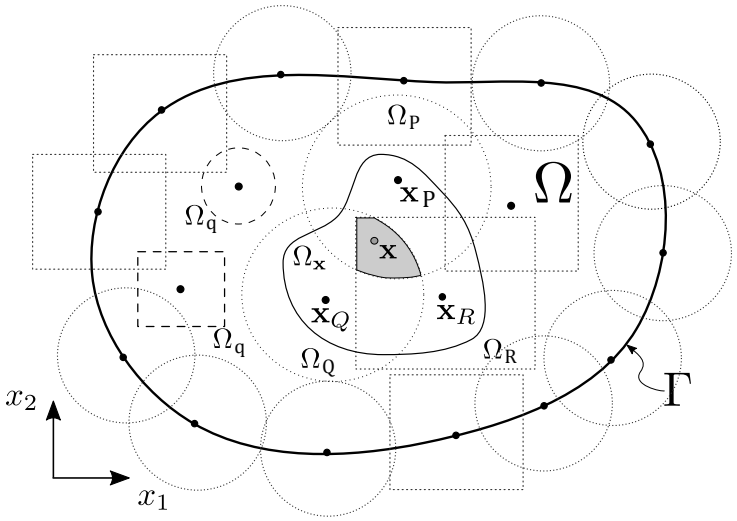

Figure 1: Representation of a global domain Ω and boundary Γ in a meshless discretization, with x_i nodes distributed within the body; Ω_s, represented as Ω_P, Ω_Q and Ω_R, is the local compact support of a node x_i, represented as x_P, x_Q and x_R; $\Omega_{\mathbf{x}}$ is the domain of definition of a sampling point x and Ω_q is the local weak-form domain or quadrature domain of a node x_i.

The coefficient vector $\mathbf{a}(\mathbf{x})$ is determined by minimizing the weighted discrete L_2 norm

$$J(\mathbf{x}) = \frac{1}{2}\sum_{i=1}^{n} w_i(\mathbf{x})\left[u^h(\mathbf{x_i}) - \hat{u}_i\right]^2 = \frac{1}{2}\sum_{i=1}^{n} w_i(\mathbf{x})\left[\mathbf{p}^T(\mathbf{x}_i)\mathbf{a}(\mathbf{x}) - \hat{u}_i\right]^2, \tag{3}$$

with respect to each term of $\mathbf{a}(\mathbf{x})$, in which $w_i(\mathbf{x})$ is the weight function associated with the node $\mathbf{x}_i$, with compact support that is $w_i(\mathbf{x}) > 0$, for all $\mathbf{x}$ in the support of $w_i(\mathbf{x})$. Figure 1 represents schematically the compact support of the MLS weight functions associated with a few nodes. Finding the extremum of $J(\mathbf{x})$ with respect to each term of $\mathbf{a}(\mathbf{x})$, leads to

$$\mathbf{A}(\mathbf{x})\mathbf{a}(\mathbf{x}) = \mathbf{B}(\mathbf{x})\hat{\mathbf{u}}, \tag{4}$$

in which

$$\mathbf{A}(\mathbf{x}) = \sum_{i=1}^{n} w_i(\mathbf{x})\mathbf{p}(\mathbf{x}_i)\mathbf{p}^T(\mathbf{x}_i), \tag{5}$$

$$\mathbf{B}(\mathbf{x}) = [w_1(\mathbf{x})\mathbf{p}(\mathbf{x}_1), w_2(\mathbf{x})\mathbf{p}(\mathbf{x}_2), \ldots, w_n(\mathbf{x})\mathbf{p}(\mathbf{x}_n)] \tag{6}$$

and

$$\hat{\mathbf{u}} = [\hat{u}_1, \hat{u}_2, \ldots, \hat{u}_n]. \tag{7}$$

Solving Eq. (4) for $\mathbf{a}(\mathbf{x})$ yields

$$\mathbf{a}(\mathbf{x}) = \mathbf{A}^{-1}(\mathbf{x})\mathbf{B}(\mathbf{x})\hat{\mathbf{u}}, \tag{8}$$

provided $n \geq m$, for each sampling point $\mathbf{x}$, as a necessary condition for a well-defined MLS approximation. In the end, substituting for $\mathbf{a}(\mathbf{x})$ into Eq. (1) results in the MLS approximation

$$u^h(\mathbf{x}) = \sum_{i=1}^{n} \phi_i(\mathbf{x})\hat{u}_i, \tag{9}$$

in which

$$\phi_i(\mathbf{x}) = \sum_{j=1}^{m} p_j(\mathbf{x}) \left[\mathbf{A}^{-1}(\mathbf{x})\mathbf{B}(\mathbf{x})\right]_{ji} \tag{10}$$

is the shape function of the MLS approximation corresponding to the node $\mathbf{x}_i$, schematically represented in Fig. 2. The MLS shape functions are not nodal interpolants that is $\phi_i(\mathbf{x}_j) \neq \delta_{ij}$.

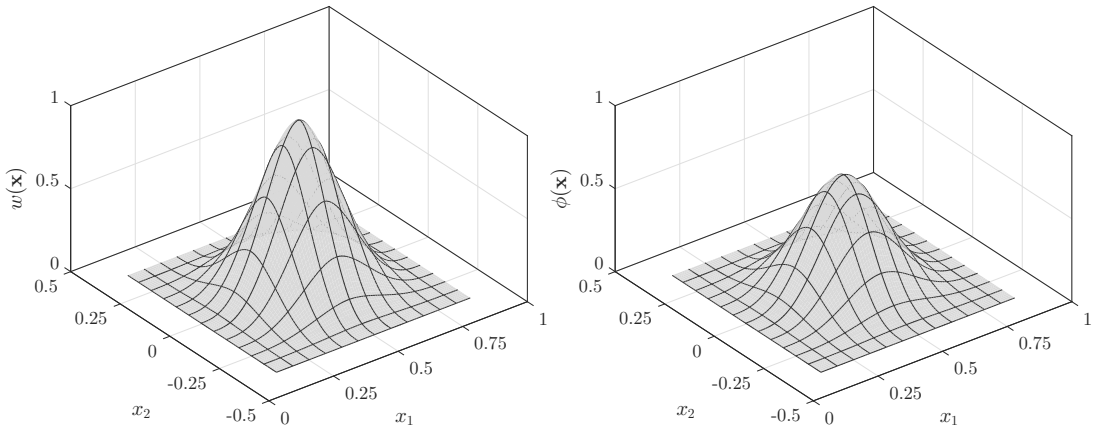

(a) Weight function (b) Shape function

Figure 2: Typical weight function and shape function of the MLS approximation

The local character of the MLS approximation is preserved, since $\phi_i(\mathbf{x})$ vanishes for $\mathbf{x}$ not in the local domain of the node $\mathbf{x}_i$. The nodal shape function is complete up to the order of the basis. Also, the smoothness of the nodal shape function is determined by the smoothness of the basis and of the weight function. The spatial derivatives of the shape function $\phi_i(\mathbf{x})$ are given by

$$\phi_{i,k} = \sum_{j=1}^{m} \left[p_{j,k}(\mathbf{A}^{-1}\mathbf{B})_{ji} + p_j(\mathbf{A}^{-1}\mathbf{B}_{,k} - \mathbf{A}^{-1}\mathbf{A}_{,k}\,\mathbf{A}^{-1}\mathbf{B})_{ji}\right], \tag{11}$$

in which $()_{,k} = \partial()/\partial x_k$.

2.2 Weight Functions

Weight functions $w_i(\mathbf{x})$, schematically represented in Fig. 2, firstly introduced in Eq. (3) for each node $\mathbf{x}_i$, have a compact support which defines the subdomain where $w_i(\mathbf{x}) > 0$, for all sampling point $\mathbf{x}$. For the sake of simplicity, this paper considers rectangular compact supports with weight functions defined as

$$w_i(\mathbf{x}) = w_{i_x}(\mathbf{x})\, w_{i_y}(\mathbf{x}) \tag{12}$$

with the weight function given by the quartic spline function

$$w_{i_x}(\mathbf{x}) = \begin{cases} 1 - 6\left(\dfrac{d_{i_x}}{r_{i_x}}\right)^2 + 8\left(\dfrac{d_{i_x}}{r_{i_x}}\right)^3 - 3\left(\dfrac{d_{i_x}}{r_{i_x}}\right)^4 & \text{for } 0 \leq d_{i_x} \leq r_{i_x} \\ 0 & \text{for } d_{i_x} > r_{i_x} \end{cases} \tag{13}$$

and

$$w_{i_y}(\mathbf{x}) = \begin{cases} 1 - 6\left(\dfrac{d_{i_y}}{r_{i_y}}\right)^2 + 8\left(\dfrac{d_{i_y}}{r_{i_y}}\right)^3 - 3\left(\dfrac{d_{i_y}}{r_{i_y}}\right)^4 & \text{for } 0 \leq d_{i_y} \leq r_{i_y} \\ 0 & \text{for } d_{i_y} > r_{i_y}, \end{cases} \tag{14}$$

in which $d_{i_x} = \|x - x_i\|$ and $d_{i_y} = \|y - y_i\|$. The parameters r_{i_x} and r_{i_y} represent the size of the support for the node i, respectively in the x and y directions.

2.3 Elastic Field

The elastic field is now approximated at a sampling point $\mathbf{x}$. Considering Eq. (9), displacement and strain components are respectively approximated as

$$\mathbf{u} = \begin{bmatrix} u^h(\mathbf{x}) \\ v^h(\mathbf{x}) \end{bmatrix} = \begin{bmatrix} \phi_1(\mathbf{x}) & 0 & \dots & \phi_n(\mathbf{x}) & 0 \\ 0 & \phi_1(\mathbf{x}) & \dots & 0 & \phi_n(\mathbf{x}) \end{bmatrix} \begin{bmatrix} \hat{u}_1 \\ \hat{v}_1 \\ \vdots \\ \hat{u}_n \\ \hat{v}_n \end{bmatrix} = \mathbf{\Phi}\,\hat{\mathbf{u}} \tag{15}$$

and

$$\boldsymbol{\varepsilon} = \mathbf{L}\,\mathbf{u} = \mathbf{L}\,\mathbf{\Phi}\,\hat{\mathbf{u}} = \mathbf{B}\,\hat{\mathbf{u}}, \tag{16}$$

in which geometrical linearity is assumed in the differential operator $\mathbf{L}$ and thus,

$$\mathbf{B} = \begin{bmatrix} \phi_{1,1} & 0 & \dots & \phi_{n,1} & 0 \\ 0 & \phi_{1,2} & \dots & 0 & \phi_{n,2} \\ \phi_{1,2} & \phi_{1,1} & \dots & \phi_{n,2} & \phi_{n,1} \end{bmatrix}. \tag{17}$$

Stress and traction components are respectively approximated as

$$\boldsymbol{\sigma} = \mathbf{D}\,\boldsymbol{\varepsilon} = \mathbf{D}\,\mathbf{B}\,\hat{\mathbf{u}} \tag{18}$$

and

$$\mathbf{t} = \mathbf{n}\,\boldsymbol{\sigma} = \mathbf{n}\,\mathbf{D}\,\mathbf{B}\,\hat{\mathbf{u}}, \tag{19}$$

in which $\mathbf{D}$ is the matrix of the elastic constants and $\mathbf{n}$ is the matrix of the components of the unit outward normal, defined as

$$\mathbf{n} = \begin{bmatrix} n_1 & 0 & n_2 \\ 0 & n_2 & n_1 \end{bmatrix}. \tag{20}$$

Equations (15) to (19) show that, at a sampling point $\mathbf{x} \in \Omega_{\mathbf{x}}$, the variables of the elastic field are defined in terms of the nodal unknowns $\hat{\mathbf{u}}$.

3 LOCAL FORM OF THE WORK THEOREM

This section present the development of the local form of the work theorem, first introduced by Oliveira and Portela (2016).

Let Ω be the domain of a body and Γ its boundary subdivided in Γ_u and Γ_t that is $\Gamma = \Gamma_u \cup \Gamma_t$, as represented in Fig. 3. The mixed fundamental boundary value problem of linear

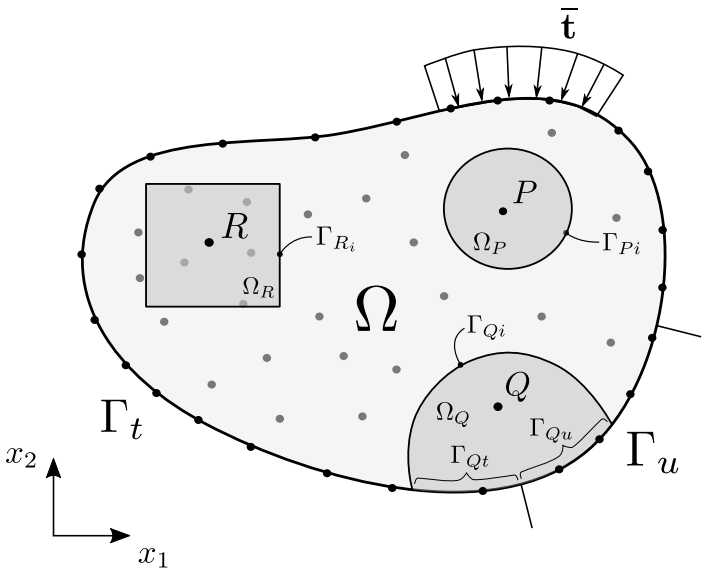

Figure 3: Meshless discretization of the global domain Ω, with boundary $\Gamma = \Gamma_u \cup \Gamma_t$; nodal points P, Q and R have corresponding local domains Ω_P, Ω_Q and Ω_R; the node Q has a local domain Ω_Q, where is defined the weighted residual associated with the node Q, with boundary $\Gamma_Q = \Gamma_{Qi} \cup \Gamma_{Qt} \cup \Gamma_{Qu}$, in which Γ_{Qi} is the interior local boundary.

elastostatics aims to determine the distribution of stresses $\boldsymbol{\sigma}$, strains $\boldsymbol{\varepsilon}$ and displacements $\mathbf{u}$ throughout the body, when it has constrained displacements $\overline{\mathbf{u}}$ defined on Γ_u and is loaded by an external system of distributed surface and body forces with densities denoted by $\overline{\mathbf{t}}$ on Γ_t and $\mathbf{b}$ in Ω, respectively.

A totally admissible elastic field is the solution of the posed problem that simultaneously satisfies the kinematic admissibility and the static admissibility. If this solution exists, see Fredholm (1906) and Fichera (2006), it can be shown that it is unique, provided linearity and stability of the material are admitted.

The general work theorem establishes an energy relationship between any statically-admissible stress field and any kinematically-admissible strain field that can be defined in the body. Derived as a weighted residual statement, the work theorem serves as a unifying basis for the formulation of numerical models in Continuum Mechanics (Brebbia, 1985).

In the domain of the body, consider a statically-admissible stress field that is

$$\mathbf{L}^T \boldsymbol{\sigma} + \mathbf{b} = \mathbf{0}, \tag{21}$$

in the domain Ω, with boundary conditions

$$\mathbf{t} = \mathbf{n}\,\boldsymbol{\sigma} = \overline{\mathbf{t}}, \tag{22}$$

on the static boundary Γ_t, in which the vector $\boldsymbol{\sigma}$ represents the stress components; $\mathbf{L}$ is a matrix differential operator; the vector $\mathbf{t}$ represent the traction components; $\overline{\mathbf{t}}$ represent prescribed values of tractions and $\mathbf{n}$ represents the outward unit normal components to the boundary.

In the global domain Ω, consider an arbitrary local subdomain Ω_Q, centered at the point Q, with boundary $\Gamma_Q = \Gamma_{Qi} \cup \Gamma_{Qt} \cup \Gamma_{Qu}$, in which Γ_{Qi} is the interior local boundary, while Γ_{Qt} and Γ_{Qu} are local boundaries that respectively share a global boundary, as represented in Fig. 3. Due to its arbitrariness, this local domain can be overlapping with other similar subdomains. For the local domain Ω_Q, the strong form of the weighted-residual equation is written as

$$\int_{\Omega_Q} \left(\mathbf{L}^T\boldsymbol{\sigma} + \mathbf{b}\right)^T \mathbf{W}_\Omega \, \mathrm{d}\Omega + \int_{\Gamma_{Qt}} \left(\mathbf{t} - \overline{\mathbf{t}}\right)^T \mathbf{W}_\Gamma \, \mathrm{d}\Gamma = \mathbf{0}, \tag{23}$$

in which $\mathbf{W}_\Omega$ and $\mathbf{W}_\Gamma$ are arbitrary weighting functions defined, respectively in Ω and on Γ. When the domain term of Eq. (23) is integrated by parts, the following local weak form of the weighted residual equation is obtained

$$\int_{\Gamma_Q} \left(\mathbf{n}\boldsymbol{\sigma}\right)^T \mathbf{W}_\Omega \, \mathrm{d}\Gamma - \int_{\Omega_Q} \left(\boldsymbol{\sigma}^T \mathbf{L}\mathbf{W}_\Omega - \mathbf{b}^T\mathbf{W}_\Omega\right) \, \mathrm{d}\Omega + \int_{\Gamma_{Qt}} \left(\mathbf{t} - \overline{\mathbf{t}}\right)^T \mathbf{W}_\Gamma \, \mathrm{d}\Gamma = \mathbf{0} \tag{24}$$

which now requires continuity of $\mathbf{W}_\Omega$, as an admissibility condition for integrability. For the sake of convenience, the arbitrary weighting function $\mathbf{W}_\Gamma$ is chosen as

$$\mathbf{W}_\Gamma = -\mathbf{W}_\Omega, \tag{25}$$

on the boundary Γ_{Qt}. Thus, Eq. (24) leads to

$$\int_{\Gamma_Q - \Gamma_{Qt}} \mathbf{t}^T\mathbf{W}_\Omega \, \mathrm{d}\Gamma + \int_{\Gamma_{Qt}} \overline{\mathbf{t}}^T\mathbf{W}_\Omega \, \mathrm{d}\Gamma - \int_{\Omega_Q} \left(\boldsymbol{\sigma}^T \mathbf{L}\mathbf{W}_\Omega - \mathbf{b}^T\mathbf{W}_\Omega\right) \, \mathrm{d}\Omega = \mathbf{0}. \tag{26}$$

Consider further an arbitrary kinematically-admissible strain field $\boldsymbol{\varepsilon}^*$, with continuous displacements $\mathbf{u}^*$ and small derivatives, in order to assume geometrical linearity, defined in the global domain that is

$$\boldsymbol{\varepsilon}^* = \mathbf{L}\,\mathbf{u}^*, \tag{27}$$

in the domain Ω, with boundary conditions

$$\mathbf{u}^* = \overline{\mathbf{u}}, \tag{28}$$

on the kinematic boundary Γ_u.

When the continuous arbitrary weighting function $\mathbf{W}_\Omega$, is defined as

$$\mathbf{W}_\Omega = \mathbf{u}^*, \tag{29}$$

the weak form (26), of the weighted residual equation, becomes

$$\int_{\Gamma_Q - \Gamma_{Qt} - \Gamma_{Qu}} \mathbf{t}^T\mathbf{u}^* \, \mathrm{d}\Gamma + \int_{\Gamma_{Qu}} \mathbf{t}^T\overline{\mathbf{u}}^* \, \mathrm{d}\Gamma + \int_{\Gamma_{Qt}} \overline{\mathbf{t}}^T\mathbf{u}^* \, \mathrm{d}\Gamma - \int_{\Omega_Q} \left(\boldsymbol{\sigma}^T \mathbf{L}\mathbf{u}^* - \mathbf{b}^T\mathbf{u}^*\right) \, \mathrm{d}\Omega = \mathbf{0} \tag{30}$$

which can be written in a compact form as

$$\int_{\Gamma_Q} \mathbf{t}^T \mathbf{u}^* \, \mathrm{d}\Gamma + \int_{\Omega_Q} \mathbf{b}^T \mathbf{u}^* \, \mathrm{d}\Omega = \int_{\Omega_Q} \boldsymbol{\sigma}^T \boldsymbol{\varepsilon}^* \, \mathrm{d}\Omega. \tag{31}$$

This equation which expresses the static-kinematic duality, is the local form of the well-known work theorem, the fundamental identity of solid mechanics, see Sokolnikoff (1956). Equation (31) is the starting point of the kinematically admissible formulations of the local meshfree methods presented in this paper.

It can be notice that the stress field $\boldsymbol{\sigma}$, is any one that satisfies equilibrium with the applied external forces $\mathbf{b}$ and $\mathbf{t}$, which is not necessarily the stress field that actually settles in the body. Also, the strain field $\boldsymbol{\varepsilon}^*$, is any one that is compatible with the constraints $\mathbf{u}^* = \overline{\mathbf{u}}$, which is not necessarily the strain field that actually settles in the body. This two fields are not linked by any constitutive relationship; indeed, they are completely independent as a consequence of the arbitrariness of the weighting function $\mathbf{W}_\Omega$. For that reason Eq. (31) can be used under the only assumption of geometrical linearity.

It is the independence of the two admissible fields of the Eq. (31) that allows the generation of different meshfree methods, when the strain field is locally defined through different options, as carried out in this paper.

A final important remark, worth of mentioning, is that the local domain Ω_Q, is any arbitrary subdomain of the global domain Ω, of the body.

4 MODELING STRATEGY

Different formulations of local meshfree methods can be derived when the arbitrary kinematically-admissible field $\boldsymbol{\varepsilon}^*$, is locally defined in the work theorem, Eq. (31). In the following sections, simple kinematically-admissible local fields will be used to derive the meshless formulation presented in this paper.

On the other hand, the statically-admissible local field $\boldsymbol{\sigma}$, will be always assumed as the elastic field that actually settles in the body. Besides satisfying static admissibility, through Eq. (21) and (22), this elastic field also satisfies kinematic admissibility defined as

$$\boldsymbol{\varepsilon} = \mathbf{L}\,\mathbf{u}, \tag{32}$$

in the domain Ω, with boundary conditions

$$\mathbf{u} = \overline{\mathbf{u}}, \tag{33}$$

on the kinematic boundary Γ_u, in which the displacements $\mathbf{u}$, are assumed continuous with small derivatives, in order to allow for geometrical linearity of the strain field $\boldsymbol{\varepsilon}$. Therefore, Eq. (33) must be enforced in the numerical model, in order to provide a unique solution of the posed problem.

For a meshless discretization of the body, the local weak-form domain or quadrature domain Ω_Q, centered at a node Q, can be defined in this paper as a rectangular or circular subdomain, as represented in Fig. 3.

5 GENERALIZED-STRAIN FORMULATION

This section briefly discuss the development of the Generalized-Strain Mesh-free (GSMF) formulation. For the complete and detailed development see Oliveira and Portela (2016).

In the local form of the work theorem, Eq. (31), the kinematically-admissible displacement field $\mathbf{u}^*$, was assumed as a continuous function leading to a regular integrable function that is the kinematically-admissible strain field $\boldsymbol{\varepsilon}^*$. However, this continuity assumption on $\mathbf{u}^*$, enforced in the local form of the work theorem, is not absolutely required but can be relaxed by convenience, provided $\boldsymbol{\varepsilon}^*$ can be useful as a generalized function, in the sense of the theory of distributions (Gelfand and Shilov, 1964). Hence, this formulation considers that the kinematically-admissible displacement field is a piecewise continuous function, defined in terms of the Heaviside step function and therefore the corresponding kinematically-admissible strain field is a generalized function, defined in terms of the Dirac delta function.

For the sake of the simplicity, in dealing with Heaviside and Dirac delta functions in a two-dimensional coordinate space, consider a scalar function d, defined as

$$d = \| \mathbf{x} - \mathbf{x}_Q \| \quad \text{that is} \quad \begin{cases} d = 0 & \text{if } \mathbf{x} \equiv \mathbf{x}_Q \\ d > 0 & \text{if } \mathbf{x} \neq \mathbf{x}_Q, \end{cases} \tag{34}$$

which represents the absolute-value function of the distance between a field point $\mathbf{x}$ and a particular reference point $\mathbf{x}_Q$, in the local domain $\Omega_Q \cup \Gamma_Q$ assigned to the field node Q. Therefore, this definition always assumes $d = d(\mathbf{x}, \mathbf{x}_Q) \geq 0$, as a positive or null value, in this case whenever $\mathbf{x}$ and $\mathbf{x}_Q$ are coincident points. It is important to remark that, in Eq. (34), neither the field point $\mathbf{x}$ nor the reference point $\mathbf{x}_Q$ is necessarily a nodal point of the local domain.

For a scalar coordinate $d \supset d(\mathbf{x}, \mathbf{x}_Q)$, the Heaviside step function can be defined as

$$H(d) = \begin{cases} 1 & \text{if } d \leq 0 \ (d = 0 \text{ for } \mathbf{x} \equiv \mathbf{x}_Q), \\ 0 & \text{if } d > 0 \text{ that is } \mathbf{x} \neq \mathbf{x}_Q, \end{cases} \tag{35}$$

in which the discontinuity is assumed at $\mathbf{x}_Q$ and consequently, the Dirac delta function is defined with the following properties

$$\delta(d) = H'(d) = \begin{cases} \infty & \text{if } d = 0 \text{ that is } \mathbf{x} \equiv \mathbf{x}_Q, \\ 0 & \text{if } d \neq 0 \ (d > 0 \text{ for } \mathbf{x} \neq \mathbf{x}_Q) \end{cases} \quad \text{and} \quad \int_{-\infty}^{+\infty} \delta(d) \, \mathrm{d}d = 1, \tag{36}$$

in which $H'(d)$ represents the distributional derivative of $H(d)$. Note that the derivative of $H(d)$, with respect to the coordinate x_i, can be defined as

$$H(d)_{,i} = H'(d) \ d_{,i} = \delta(d) \ d_{,i} = \delta(d) \ n_i. \tag{37}$$

Since the result of this equation is not affected by any particular value of the constant n_i, this constant will be conveniently redefined later on.

Kronecker delta function can be defined through Heaviside step function as

$$\Delta(d) = H(d) - H(-d) + 1 = \begin{cases} 1 & \text{if } d = 0 \text{ that is } \mathbf{x} \equiv \mathbf{x}_Q, \\ 0 & \text{if } d > 0 \text{ that is } \mathbf{x} \neq \mathbf{x}_Q, \end{cases} \tag{38}$$

which has the distributional derivative always null that is

$$\Delta'(d) = \delta(d) - \delta(-d) = \delta(d) - \delta(d) = 0, \tag{39}$$

as a consequence of the symmetry of Dirac delta function.

Now consider that d_l, d_j and d_k represent the distance function d, defined in Eq. (34), for corresponding field points $\mathbf{x}_l$, $\mathbf{x}_j$ and $\mathbf{x}_k$. Then, the kinematically-admissible displacement field can be defined as a linear combination of Kronecker delta function evaluations at an arbitrary number of collocation points, conveniently arranged in the local domain $\Omega_Q \cup \Gamma_Q$ of the field node Q, that is

$$\mathbf{u}^*(\mathbf{x}) = \left[\frac{L_i}{n_i} \sum_{l=1}^{n_i} \Delta(d_l) + \frac{L_t}{n_t} \sum_{j=1}^{n_t} \Delta(d_j) + \frac{S}{n_\Omega} \sum_{k=1}^{n_\Omega} \Delta(d_k) \right] \mathbf{e}, \tag{40}$$

in which $\mathbf{e} = [1 \;\; 1]^T$ represents the metric of the orthogonal directions; n_i, n_t and n_Ω represent the number of collocation points, respectively on the local interior boundary $\Gamma_{Qi} = \Gamma_Q - \Gamma_{Qt} - \Gamma_{Qu}$ with length L_i, on the local static boundary Γ_{Qt} with length L_t and in the local domain Ω_Q with area S. This assumed displacement field $\mathbf{u}^*(\mathbf{x})$, a discrete rigid-body unit displacement defined at collocation points, schematically represented in Fig. 4, conveniently leads to a null

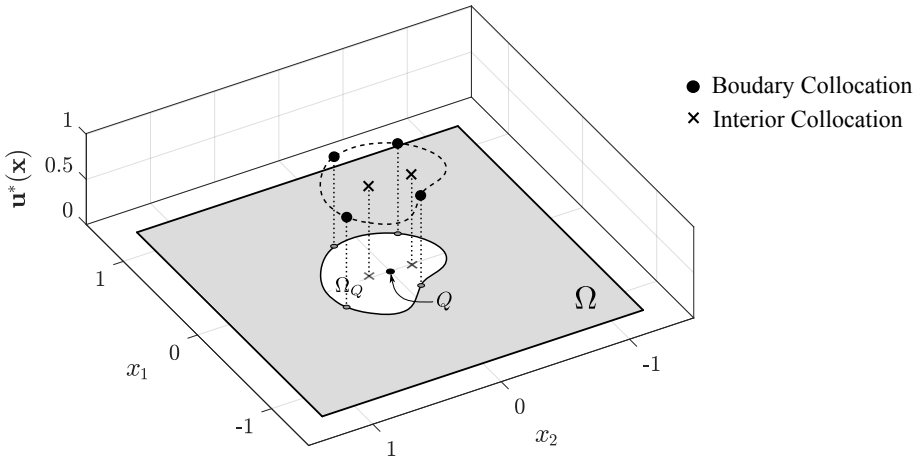

Figure 4: Schematic representation of the displacement $\mathbf{u}^*(\mathbf{x})$ of Eq. (40), a discrete rigid-body unit displacement defined at collocation points, of the Generalized-Strain Mesh-free formulation, for a local domain associated with a field node Q.

generalized strain field that is

$$\boldsymbol{\varepsilon}^*(\mathbf{x}) = \mathbf{0}, \tag{41}$$

as a consequence of Eq. (39). The local work theorem, Eq. (31), can be written as

$$\int_{\Gamma_Q - \Gamma_{Qt}} \mathbf{t}^T \mathbf{u}^* \, \mathrm{d}\Gamma + \int_{\Gamma_{Qt}} \bar{\mathbf{t}}^T \mathbf{u}^* \, \mathrm{d}\Gamma + \int_{\Omega_Q} \mathbf{b}^T \mathbf{u}^* \, \mathrm{d}\Omega = \int_{\Omega_Q} \boldsymbol{\sigma}^T \boldsymbol{\varepsilon}^* \, \mathrm{d}\Omega \tag{42}$$

which, after considering the assumed displacement and the strain components of the kinematically-admissible field, respectively Eq. (40) and (41), leads to

$$\frac{L_i}{n_i} \sum_{l=1}^{n_i} \int_{\Gamma_Q - \Gamma_{Qt}} \mathbf{t}^T \Delta(d_l) \, \mathbf{e} \, \mathrm{d}\Gamma + \frac{L_t}{n_t} \sum_{j=1}^{n_t} \int_{\Gamma_{Qt}} \bar{\mathbf{t}}^T \Delta(d_j) \, \mathbf{e} \, \mathrm{d}\Gamma + \frac{S}{n_\Omega} \sum_{k=1}^{n_\Omega} \int_{\Omega_Q} \mathbf{b}^T \Delta(d_k) \, \mathrm{d}\Omega = 0. \tag{43}$$

Now considering the properties of Kronecker delta function, defined in Eq. (38), the Eq. (43) simply leads to

$$\mathbf{e}^T \left[\frac{L_i}{n_i} \sum_{l=1}^{n_i} \mathbf{t}_{\mathbf{x}_l} + \frac{L_t}{n_t} \sum_{j=1}^{n_t} \bar{\mathbf{t}}_{\mathbf{x}_j} + \frac{S}{n_\Omega} \sum_{k=1}^{n_\Omega} \mathbf{b}_{\mathbf{x}_k} \right] = 0 \tag{44}$$

and finally to

$$\frac{L_i}{n_i} \sum_{l=1}^{n_i} \mathbf{t}_{\mathbf{x}_l} = -\frac{L_t}{n_t} \sum_{j=1}^{n_t} \bar{\mathbf{t}}_{\mathbf{x}_j} - \frac{S}{n_\Omega} \sum_{k=1}^{n_\Omega} \mathbf{b}_{\mathbf{x}_k}. \tag{45}$$

Equation (45) states the equilibrium of tractions and body forces, pointwisely defined at collocation points, as schematically represented in Fig. 5; obviously, the pointwise version of the

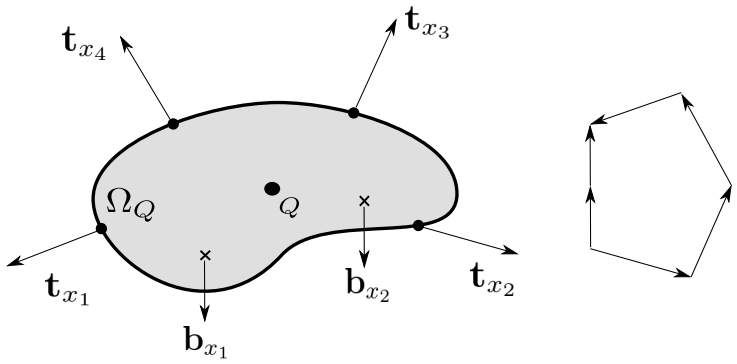

Figure 5: Schematic representation of the equilibrium of tractions and body forces, of Eq. (45), pointwisely defined at collocation points of a local domain associated with a field node Q, of the Generalized-Strain Mesh-free formulation.

Euler - Cauchy stress principle. This is the equation used in the Generalized-Strain Mesh-free (GSMF) formulation which, therefore, is free of integration. Since the work theorem is a weighted-residual weak form, it can be easily seen that this integration-free formulation is nothing else other than a weighted-residual weak-form collocation.

Equations (45), of the Generalized-Strain Mesh-free formulation, can be derived from another kinematically-admissible displacement field, directly defined in terms of Heaviside step function, see Oliveira and Portela (2016).

Discretization of Eq. (45) is carried out with the MLS approximation, Eq. (15) to (19), for the local domain Ω_Q, in terms of the nodal unknowns $\hat{\mathbf{u}}$, thus leading to the system of two linear algebraic equations

$$\frac{L_i}{n_i} \sum_{l=1}^{n_i} \mathbf{n}_{\mathbf{x}_l} \mathbf{D} \mathbf{B}_{\mathbf{x}_l} \hat{\mathbf{u}} = -\frac{L_t}{n_t} \sum_{j=1}^{n_t} \bar{\mathbf{t}}_{\mathbf{x}_j} - \frac{S}{n_\Omega} \sum_{k=1}^{n_\Omega} \mathbf{b}_{\mathbf{x}_k} \tag{46}$$

that can be written as

$$\mathbf{K}_Q \, \hat{\mathbf{u}} = \mathbf{F}_Q, \tag{47}$$

in which $\mathbf{K}_Q$, the nodal stiffness matrix associated with the local domain Ω_Q, is a $2 \times 2n$ matrix given by

$$\mathbf{K}_Q = \frac{L_i}{n_i} \sum_{l=1}^{n_i} \mathbf{n}_{\mathbf{x}_l} \mathbf{D} \mathbf{B}_{\mathbf{x}_l} \tag{48}$$

and $\mathbf{F}_Q$ is the respective force vector given by

$$\mathbf{F}_Q = -\frac{L_t}{n_t} \sum_{j=1}^{n_t} \bar{\mathbf{t}}_{\mathbf{x}_j} - \frac{S}{n_\Omega} \sum_{k=1}^{n_\Omega} \mathbf{b}_{\mathbf{x}_k} \tag{49}$$

Consider that the problem has a total of N field nodes Q, each one associated with the respective local region Ω_Q. Assembling Eq. (47), for all M interior and static–boundary field nodes leads to the global system of $2M \times 2N$ equations

$$\mathbf{K}\,\hat{\mathbf{u}} = \mathbf{F}. \tag{50}$$

Finally, the remaining equations are obtained from the $N - M$ boundary field nodes on the kinematic boundary. For a field node on the kinematic boundary, a direct interpolation method is used to impose the kinematic boundary condition as

$$u_k^h(\mathbf{x}_j) = \sum_{i=1}^{n} \phi_i(\mathbf{x}_j) \hat{u}_{ik} = \overline{\mathbf{u}}_k, \tag{51}$$

or, in matrix form as

$$\mathbf{u}_k = \mathbf{\Phi}_k\,\hat{\mathbf{u}} = \overline{\mathbf{u}}_k, \tag{52}$$

with $k = 1, 2$, where $\overline{\mathbf{u}}_k$ is the specified nodal displacement component. Equations (51) are directly assembled into the global system of equations (50).

6 NUMERICAL RESULTS

This section presents some numerical results comparing the Generalized-Strain Mesh-free (GSMF) formulation with the Rigid-Body Displacement Mesh-free (RBDMF) formulation, the Element-free Galerkin (EFG) and the Meshless Local Petrov–Galerkin Finite Volume Method (MLPG FVM).

For a generic node i, the size of the local support Ω_s and the local domain of integration Ω_q are respectively given by

$$r_{\Omega_s} = \alpha_s\, c_i, \tag{53}$$

and

$$r_{\Omega_q} = \alpha_q\, c_i, \tag{54}$$

in which c_i represents the distance of the node i, to the nearest neighboring node; for the applications presented in this paper, $\alpha_s = 3.0 \sim 4.5$ and $\alpha_q = 0.5 \sim 0.6$ were used. Only local

meshless methods like the RBDMF, the GSMF and the MLPG FVM use local domains; the EFG use background cells for integration purpose.

Displacement and energy norms can be used for error estimation. These norms can be computed, respectively as

$$\|\mathbf{u}\| = \left[\int_{\Omega} \mathbf{u}^T\mathbf{u}\,\mathrm{d}\Omega\right]^{1/2} \tag{55}$$

and

$$\|\boldsymbol{\varepsilon}\| = \left[\frac{1}{2}\int_{\Omega} \boldsymbol{\varepsilon}^T\mathbf{D}\,\boldsymbol{\varepsilon}\,\mathrm{d}\Omega\right]^{1/2}. \tag{56}$$

The relative error for $\|\mathbf{u}\|$ and $\|\boldsymbol{\varepsilon}\|$ is given, respectively by

$$r_u = \frac{\|\mathbf{u}_{num} - \mathbf{u}_{exact}\|}{\|\mathbf{u}_{exact}\|} \tag{57}$$

and

$$r_\varepsilon = \frac{\|\boldsymbol{\varepsilon}_{num} - \boldsymbol{\varepsilon}_{exact}\|}{\|\boldsymbol{\varepsilon}_{exact}\|}. \tag{58}$$

6.1 Cantilever Beam

Consider a beam of dimensions $L \times D$ and of unit depth, subjected to a parabolic traction at the free end as shown in Fig. 6. The beam is assumed in a plane stress state and the parabolic

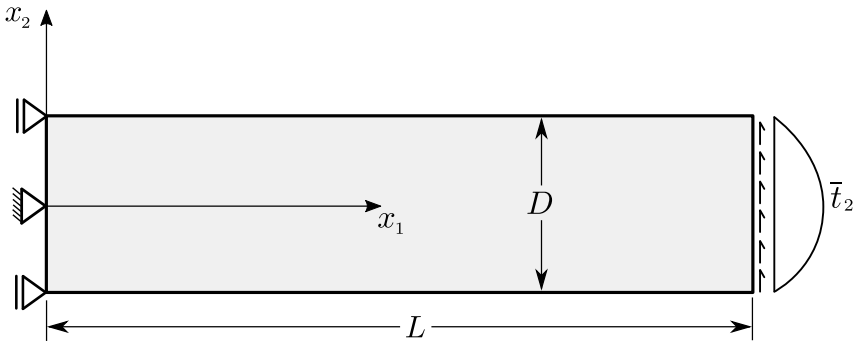

Figure 6: Timoshenko cantilever beam.

traction is given by

$$\overline{t}_2(x_2) = -\frac{P}{2I}\left(\frac{D^2}{4} - x_2^2\right), \tag{59}$$

where $I = D^3/12$ is the moment of inertia. The exact displacement components for this problem are given by

$$u_1(x_1, x_2) = -\frac{Px_2}{6EI}\left[(6L - 3x_1)x_1 + (2+\nu)\left(x_2^2 - \frac{D^2}{4}\right)\right] \tag{60}$$

and

$$u_2(x_1,x_2)=\frac{P}{6EI}\left[3\nu x_2^2(L-x_1)+(4+5\nu)\frac{D^2x_1}{4}+(3L-x_1)x_1^2\right] \tag{61}$$

and the exact stress components are given by

$$\sigma_{11}(x_1,x_2)=-\frac{P(L-x_1)x_2}{I},\quad \sigma_{12}(x_1,x_2)=-\frac{P}{2I}\left(\frac{D^2}{4}-x_2^2\right)\ \text{ and }\ \sigma_{22}(x_1,x_2)=0. \tag{62}$$

Material properties are taken as Young′s modulus $E=3.0\times10^7$ and the Poisson′s ratio $\nu=0.3$ and the beam dimensions are $D=12$ and $L=48$. The shear force is $P=1000$. To solve this problem, a regular nodal distribution, represented in Fig. 7, was considered with a

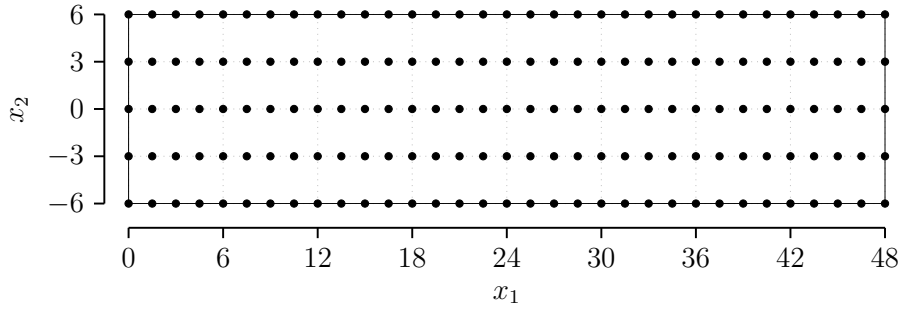

Figure 7: The regular nodal distribution of the cantilever-beam discretization.

discretization of $33\times5=165$ nodes.

For the local kinematic formulations rectangular local domains were considered, with 1 collocation point to compute the weak form of GSMF and 10 Gauss-quadrature points to integrate the weak-form of RBDMF, placed on each boundary of the local domain. The EFG considered 10 Gauss-quadrature points on each background cell and the MLPG FVM considered 10 Gauss-quadrature points distributed on the local domain. A first-order polynomial basis was considered in MLS approximation.

The weak-form collocation of GSMF represents a clear reduction of the computational effort when compared to other meshless methods. The GSMF require only 1 collocation point, placed on each boundary of the local domain, to obtain the most accurate results, see Oliveira and Portela (2016), while the other methods require at least 10 Gauss-quadrature points in order to obtain a good accuracy. This important feature is measure through CPU time consumption and convergence rates.

The displacements obtained with the four methods, represented in Fig. 8, show very good agreement with the results of the exact solution, although the MLPG FVM is slightly less accurate than the others. In this initial analysis, the fastest computation is obtained with the GSMF, which is 21% faster than the MLPG FVM, the second best result.

In order to further the study of the computational efficiency of the presented method, three regular discretizations of the cantilever-beam, with $65\times9=585$, $97\times13=1261$ and $129\times17=2193$ nodes were considered. Only the major computational cost that is the cost of generating the global stiffness matrix and solving the system of algebraic equations, was measured. All the

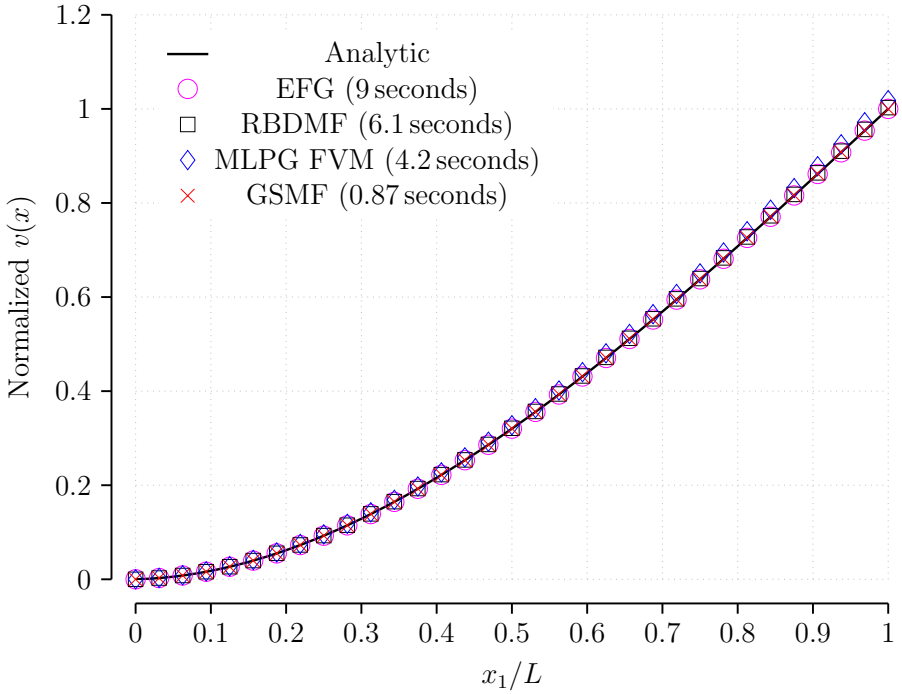

Figure 8: Normalized displacements of the cantilever-beam discretization with 165 nodes.

routines were compared when using MATLAB 2015a on an Intel Core I7-4700MQ computer with CPU of 2.4GHz and 16 GB of RAM.

The results obtained are presented in Fig. 9, where it can be seen that CPU time of GSMF

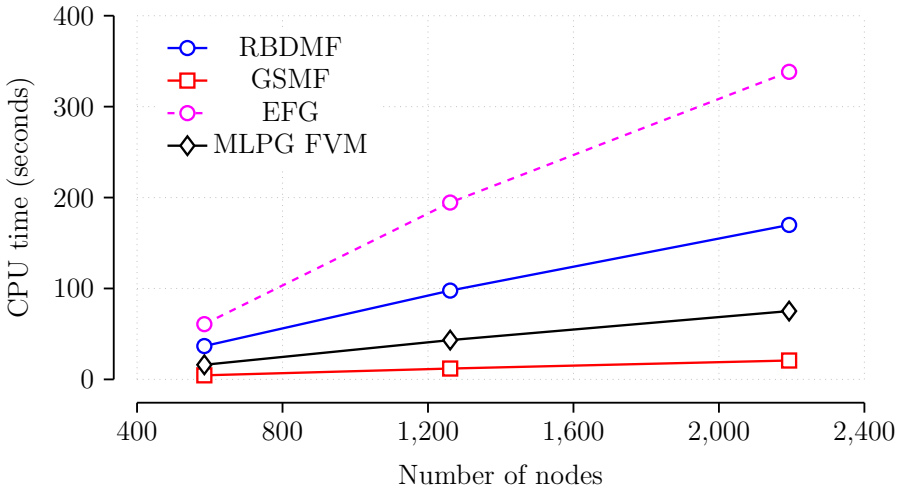

Figure 9: CPU time consumption of a cantilever-beam with 585, 1261 and 2193.

is always much lower than CPU time of the other methods, using the same parameters. The CPU time consumption of the GSMF is 28% faster than the second best value that is the one obtained with the MLPG FVM. This important result clearly evidences the high computational efficiency of GSMF.

Another test was performed to assess the accuracy and convergence of the analyzed meth-

ods, using the relative energy norm. Since the MLPG FVM obtained the least accurate result among all methods, it was not compared in this test. Three regular discretizations with $65 \times 9 = 585$, $97 \times 13 = 1261$ and $129 \times 17 = 2193$ nodes were considered. Figure 10 presents

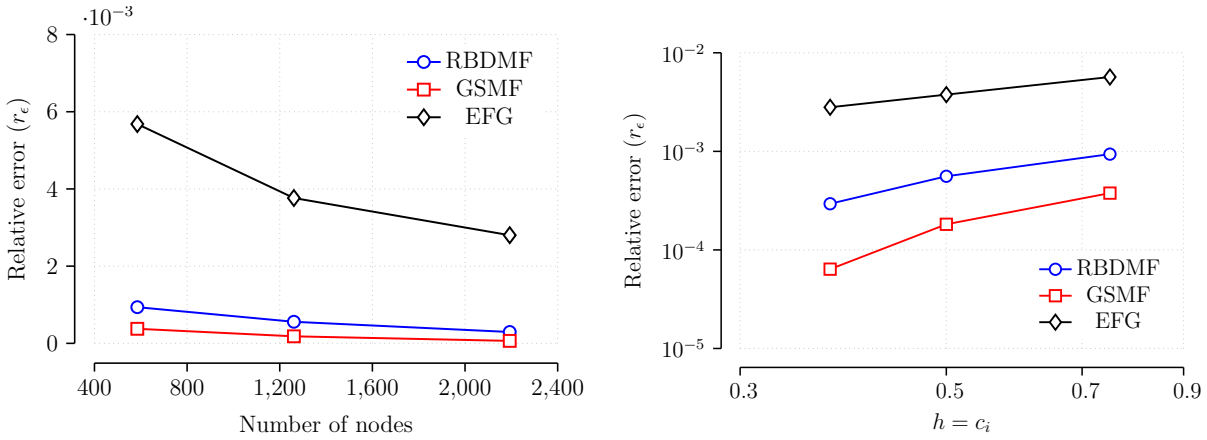

(a) Accuracy.

(b) Convergence rates.

Figure 10: Accuracy and convergence rates for the cantilever-beam discretization with 585, 1261 and 2193 nodes; c_i is the distance of a generic node i, to the nearest neighboring node, as defined in Eq. (53) and (54).

the results obtained for the accuracy and convergence rates. The results show that the GSMF is more accurate than the RBDMF and the EFG, with better convergence rates when compared to both of them.

CONCLUSIONS

A numerical comparison of the weak-form collocation and three meshless methods is performed, for the solution of two-dimensional problems in linear elasticity.

The Rigid-body Displacement Mesh-free (RBDMF) formulation, the Element-free Galerkin (EFG) and the Meshless Local Petrov-Galerkin Finite Volume Method (MLPG FVM) rely on integration and quadrature process to obtain the stiffness matrix; while the Generalized-Strain Mesh-free (GSMF) formulation is completely integration free, working as a weighted-residual weak-form collocation.

A numerical example was analyzed with these methods, in order to compare the accuracy and the computational effort, using the same parameters. The results obtained with all methods are in agreement with those of the available analytical solution. The MLPG FVM led to very fast computations, although obtained the least accurate results among all methods. The EFG and the RBDMF obtained very accurate results with a good convergence rate, but are computationally more expensive than the other methods. Among all methods, the GSMF obtained the most accurate results with the fastest computation.

All the numerical results obtained clearly demonstrate that this weighted-residual weak-form collocation readily overcomes the well-known difficulties posed by the weighted-residual strong-form collocation, regarding accuracy and stability of the solution. The results obtained using only 1 collocation point led to accurate results with incredible fast computations, surpassing all the other analyzed methods. This features make the GSMF superior when compared to

the other meshless methods presented in this paper, making it a robust formulation for solving two-dimensional problems in linear elasticity.

ACKNOWLEDGEMENTS

The first author acknowledges the program *PECC – Pós-Graduação em Estruturas e Construção Civil*, Department of Civil Engineering, Faculty of Technology, University of Brasília and *CNPq – Brazilian National Counsel of Technological and Scientific Development* for his Masters scholarship.

REFERENCES

Atluri, S.N. and S. Shen (2002). "The Meshless Local Petrov-Galerkin (MLPG) Method: A Simple and Less-costly Alternative to the Finite Element and Boundary Element Methods". In: *CMES: Computer Modeling in Engineering and Sciences* 3.1, pp. 11–51.

Atluri, S.N. and T. Zhu (1998). "A new Meshless Local Petrov-Galerkin (MLPG) approach in computational mechanics". In: *Computational Mechanics* 22.2, pp. 117–127.

Atluri, S.N., Z.D. Han, and A.M. Rajendran (2004). "A New Implementation of the Meshless Finite Volume Method Through the MLPG Mixed Approach". In: *CMES: Computer Modeling in Engineering and Sciences* 6, pp. 491–513.

Belytschko, T., Y. Y. Lu, and L. Gu (1994). "Element-free Galerkin methods". In: *International Journal for Numerical Methods in Engineering* 37.2, pp. 229–256. ISSN: 1097-0207.

Brebbia, C.A. and H. Tottenham, eds. (1985). *Variational Basis of Approximate Models in Continuum Mechanics*. The II International Conference on Variational Methods in Engineering. Berlin: Southampton and Springer Verlag.

Fichera, G (2006). *Linear Elliptic Differential Systems and Eigenvalue Problems*. Springer.

Finalyson, B.A. (1972). *The Method of Weighted Residuals and Variational Principles*. Vol. 87. Academic Press, p. 472.

Fredholm, I. (1906). "Solution d'un problme fondamental de la thorie de l'lasticit". In: *Arkiv fr Matematik Astronomi och Fysk 2* 28.1, pp. 1–8.

Gelfand, I.M. and G.E. Shilov (1964). *Generalized Functions*. Vol. 1. Academic Press.

Liu, G.R. and Y.T. Gu (2001). "A Local Point Interpolation Method for Stress Analysis of Two-Dimensional Solids". In: *Structural Engineering and Mechanics* 11.2, 221–236.

Liu, G.R. et al. (2002). "Point Interpolation Method Based on Local Residual Formulation Using Radial Basis Functions". In: *Structural Engineering and Mechanics* 14, 713–732.

Liu, W.K., S. Jun, and Y.F. Zhang (1995). "Reproducing Kernel Particle Methods". In: *International Journal for Numerical Methods in Engineering* 20, 1081–1106.

Nayroles, B., G. Touzot, and P. Villon (1992). "Generalizing the Finite Element Method: Diffuse Approximation and Diffuse Elements". In: *Computational Mechanics* 10, 307–318.

Oliveira, T. and A. Portela (2016). "Weak-Form Collocation – a Local Meshless Method in Linear Elasticity". Engineering Analysis with Boundary Elements. Submitted.

Sokolnikoff, I. S. (1956). *Mathematical theory of elasticity*. Vol. 83. McGraw-Hill New York.

Zhu, T., J. Zhang, and S.N. Atluri (1998). "A Local Boundary Integral Equation (LBIE) Method in Computational Mechanics and a Meshless Discretization Approach". In: *Computational Mechanics* 21, 223–235.